

# Study of a lipophilic captopril analogue binding to angiotensin I converting enzyme

Georgios A. Dalkas,<sup>a</sup> Damien Marchand,<sup>b</sup> Jean-Claude Galleyrand,<sup>b</sup> Jean Martinez,<sup>b</sup> Georgios A. Spyroulias,<sup>a\*</sup> Paul Cordopatis<sup>a</sup> and Florine Cavalier<sup>b\*</sup>

Human ACE is a central component of the renin–angiotensin system and a major therapeutic target for cardiovascular diseases. The somatic form of the enzyme (sACE) comprises two homologous metallopeptidase domains (N and C), each bearing a zinc active site with similar but distinct substrate and inhibitor specificities. In this study, we present the biological activity of silacaptopril, a silylated analogue of captopril, and its binding affinity towards ACE. Based on the recently determined crystal structures of both the ACE domains, a series of docking calculations were carried out in order to study the structural characteristics and the binding properties of silacaptopril and its analogues with ACE. Copyright © 2009 European Peptide Society and John Wiley & Sons, Ltd.

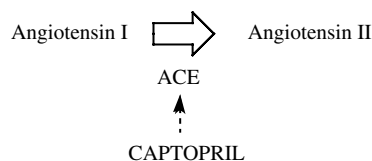
**Keywords:** ACE; zinc metalloenzyme; silacaptopril; docking simulations

## Introduction

The ACE, a zinc metalloenzyme, plays a fundamental role in blood pressure regulation by converting the inactive decapeptide angiotensin I to a potent vasopressor octapeptide angiotensin II. Two isoforms of ACE transcribed from the same gene in a tissue-specific manner [1]: the somatic form (sACE), which is found in a variety of tissues, and the testicular form (tACE), which is expressed in germinal cells exclusively. sACE is a 1277-residue type I transmembrane glycoprotein with an ectodomain consisting of two highly homologous domains (N and C domains). tACE is a 701-amino-acid isoform identical to the C domain of sACE [2], except for the first 36 residues. Each domain contains an active site bearing the characteristic HEXXH zinc-binding motif of Zn-peptidases (zincins) [3].

The recent breakthrough in determining the high-resolution crystal structures of human tACE (C domain of sACE) [4,5] and that of the N domain of sACE [6], both in the absence and presence of the potent inhibitor lisinopril, has renewed the interest in studying their enzymatic activity at a molecular level and has provided a structural basis for the design of domain-specific inhibitors [7,8]. Despite the structural homology of the two domains of sACE, which have ~60% sequence identity, some notable differences between the active sites were observed [6]. Consistent with the observed chloride-dependent activation of ACE [9], only one chloride ion was bound to the N domain as opposed to the two found in the crystal structure of tACE [6,10].

Drug design based on peptide structure–activity relationships is an area of great importance [11]. The knowledge of an enzyme belonging to a defined family and the analogy with other proteins is often used to assist the design of new potential inhibitors [12–14]. Captopril, a competitive inhibitor of ACE, is currently used as an oral anti-hypertensive agent (Scheme 1) [15–18]. Taking into consideration that the captopril's methyl group (Scheme 2) contributes to the inhibitory potency, possibly via a hydrophobic interaction with the enzyme, we aim to



**Scheme 1.** Role of ACE.

further enhance the importance of the hydrophobic interaction of the proline moiety. Modifications of the proline ring-like bicyclopropane or bicyclopentane have been performed [19].

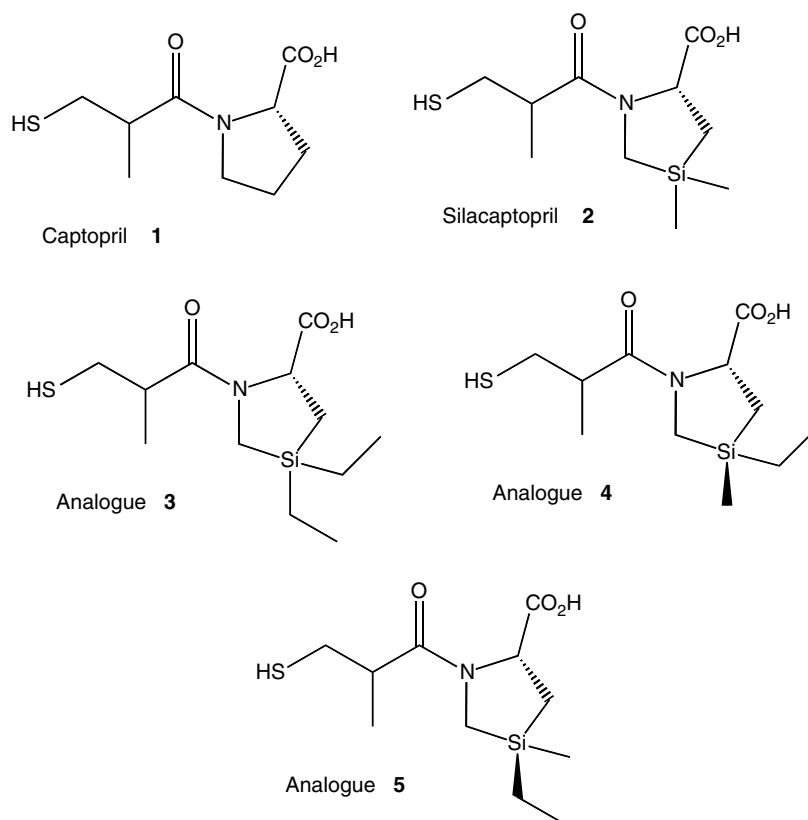
Regarding our contribution, the proline was replaced with the more lipophilic surrogate 4'-dimethylsilaprolinone [20], in order to increase the lipophilicity of captopril, while conserving the inhibitory activity, since the conformational features of captopril structural core will be preserved. The introduction of a di-substituted silicon atom attenuates the hydrophilic character of the molecule and could enhance hydrophobic interactions with ACE. Additionally, three new analogues of di-substituted silacaptopril have been designed and tested *in silico* for their binding affinity and posing into the Zn catalytic site through docking simulations.

\* Correspondence to: Georgios A. Spyroulias, Department of Pharmacy, University of Patras, Panepistimioupoli – Rion, GR-26504, Greece. E-mail: G.A.Spyroulias@upatras.gr

\* Florine Cavalier, IBMM, UMR CNRS-UM1-UM2 5247, Université Montpellier 2, Place Eugène Bataillon, 34095 Montpellier cedex, France. E-mail: florine@univ-montp2.fr

a Department of Pharmacy, University of Patras, Panepistimioupoli – Rion, GR-26504, Greece

b IBMM, UMR CNRS-UM1-UM2 5247, Université Montpellier 2, Place Eugène Bataillon, 34095 Montpellier cedex, France



**Scheme 2.** Structure of captopril and analogues.

## Materials and Methods

### Synthesis

#### 3-bromo-2-methylpropionic acid **6**

HBr gas was bubbled for 2 h in a solution of metacrylic acid (5 ml, 58 mM) at room temperature. The reaction mixture was purified by Kugelrohr distillation under reduced pressure to afford the title compound as a colourless oil; (70%) **Rf**: 0.75 (CHCl<sub>3</sub>/MeOH/AcOH 120/10/5) m.p. 106–108 °C/15 mbar; RMN<sup>1</sup>H (CDCl<sub>3</sub>)  $\delta$  = 1.35 (d  $J$  = 7 Hz, 3H, CH<sub>3</sub>), 3.00 (m, 1H, CH), 3.60 (m, 2 H, CH<sub>2</sub>Br).

#### Compound **8**

A mixture of 3-bromo-2-methylpropionic acid **6** (177 mg, 1.066 mM) containing two drops of DMF in CH<sub>2</sub>Cl<sub>2</sub> was stirred. Oxalyl chloride (140  $\mu$ l, 1.5 eq, 1.6 mM) was added slowly and stirring at room temperature was continued until gas evolution substantially slowed. An additional portion of oxalyl chloride (26  $\mu$ l, 1/3 eq, 0.3 mM) was added, and when gas evolution ceased, the mixture was concentrated in vacuo. Twice, portions of cyclohexane (2 ml) were added and evaporated in vacuo.

The residue was dissolved in THF (3 ml), then a solution of (L)-silaproline methyl ester hydrochloride **7** (200 mg, 0.954 mM) in THF (3 ml) and propylene oxide (267 ml, 3.82 mM) were added and the reaction was stirred for 3 h at 50 °C in a sealed system. The solvent was removed and the residue purified by flash chromatography on silica gel. The relevant fractions yielded the expected compound **8** as an oil (87%).

**Rf**: 0.3 (AcOEt/hexane 3/7);

**SM-ESI**  $+$ : 322–324 [M+H]<sup>+</sup>, 643–647 [2 M+H]<sup>+</sup>;

**RMN<sup>1</sup>H (CDCl<sub>3</sub>)**: (2 diastereoisomers)  $\delta$  = 0.29 and 0.31 (2 s, 12 H, 2  $\times$  Si(CH<sub>3</sub>)<sub>2</sub>), 1.15–1.40 (m, 4 H, 2  $\times$  CH<sub>2</sub>CH<sub>2</sub>Si), 1.25 and 1.28 (2d  $J$  = 6.4 Hz, 6.7 Hz, 6 H, 2  $\times$  CH<sub>3</sub>CHCO), 2.89 and 3.02 (2d  $J$  = 13.2 Hz, 13.3 Hz, 1 H, NCHHSi), 3.04 and 3.06 (2d  $J$  = 13.3 Hz, 13.2 Hz, 1 H, NCHHSi), 2.25–2.40 (m, 4 H, BrCH<sub>2</sub>), 3.65–3.75 (m, 2 H, CH<sub>3</sub>CHCO), 3.72 and 3.73 (2 s, 6 H, 2  $\times$  OCH<sub>3</sub>), 5.00–5.10 (2dd  $J$  = 4 Hz, 9.8 Hz, 2 H, CH<sub>2</sub>).

#### Ac-Silacaptopril-OMe (R/S, R) **9**

Compound **8** (200 mg, 0.621 mM) was dissolved in acetone (1.2 ml), and potassium thioacetate (142 mg, 1.242 mM) was added. The reaction mixture was refluxed overnight. After removal of acetone, the resulting residue was purified by flash chromatography on silica gel (84%).

**Rf**: 0.4 (AcOEt/hexane 3/7);

**SM-ESI**  $+$ : 318–320 [M+H]<sup>+</sup>;

**RMN<sup>1</sup>H (CDCl<sub>3</sub>)**: (2 diastereoisomers)  $\delta$  = 0.21 and 0.24 (2 s, 12 H, 2  $\times$  Si(CH<sub>3</sub>)<sub>2</sub>), 1.10–1.30 (m, 4 H, 2  $\times$  CH<sub>2</sub>CH<sub>2</sub>Si), 1.15 and 1.20 (2d  $J$  = 6.4 Hz, 6.7 Hz, 6 H, 2  $\times$  CH<sub>3</sub>CHCO), 2.27 and 2.29 (2 s, 6 H, CH<sub>3</sub>COS), 2.78–3.19 (m, 10 H, SCH<sub>2</sub>, CH<sub>3</sub>CHCO, NCH<sub>2</sub>Si), 3.65 and 3.67 (2 s, 6 H, 2  $\times$  OCH<sub>3</sub>), 4.90–5.00 (2dd  $J$  = 4 Hz, 9.8 Hz, 2 H, CH<sub>2</sub>).

#### Silacaptopril (R/S,R) **2**

The fully protected silacaptopril **9** (100 mg, 0.315 mM) was dissolved in degassed solvents (THF/H<sub>2</sub>O : 10/1) (10 ml). Lithium hydroxide (20.2 mg, 2.523 mM) was then added and the reaction was monitored by HPLC. When all starting materials disappeared, 12N HCl was added and the aqueous phase was extracted with

EtOAc. The combined organic phases were dried over  $\text{MgSO}_4$ , filtered and concentrated *in vacuo* to afford the title compound in 85% yield.

**Rf:** 0.6 ( $\text{CHCl}_3/\text{MeOH}/\text{AcOH}$  120/10/5)

**SM-ESI**  $+$ : 262–264  $[\text{M}+\text{H}]^+$ ;

**RMN<sup>1</sup>H (CDCl<sub>3</sub>):** (2 diastereoisomers)  $\delta$  = 0.32–0.38 (m, 12 H,  $2 \times \text{Si}(\text{CH}_3)_2$ ), 1.20–1.30 (m, 8 H,  $2 \times \text{CH}_3\text{CHCO}$  and  $2 \times \text{HSCH}_2$ ), 1.40–1.70 (m, 4 H,  $\text{CH}_2\text{CH}_2\text{Si}$ ), 2.85–3.20 (m, 10 H,  $\text{SCH}_2$  and  $\text{CH}_3\text{CHCO}$  and  $\text{NCH}_2\text{Si}$ ), 5.05–5.20 (m, 2 H,  $\text{CH}_\alpha$ ), 6.00–6.70 (bs, 2 H,  $\text{CO}_2\text{H}$ ).

### Biological Assays

Lyophilized ACE was restored in distilled water and stored at  $-80^\circ\text{C}$  until tested. The substrate was the tripeptide Hip-His-Leu-OH. ACE activity was measured by using the fluorimetric method of Santos *et al.* with slight modifications [21].

Briefly, the enzymatic hydrolysis of the substrate ( $3.5 \times 10^{-4}$  M) was carried out for 1 h at  $37^\circ\text{C}$  in 50 mM Tris HCl pH 8.3 containing NaCl 0.3 M (final volume 100  $\mu\text{l}$ ) [22] in the presence of 0.005 U of ACE (2.2 ng). These conditions provided constant velocity and optimal enzymatic activity.

The enzyme reaction was stopped by adding 400  $\mu\text{l}$  of 2N NaOH and 3 ml of distilled water. A measured quantity of 0.1 ml of 1% (w/v) 1,2-benzenedicarboxaldehyde in methanol was added in the alkalinized mixture. After exactly 4 min, 0.2 ml of 6N HCl was added. The fluorescence of the mixtures was measured with excitation at 365 nm and emission at 495 nm.

### Computational Methods

#### Structure preparation

The crystal structure coordinates of ACE were obtained from the Protein Data Bank (PDB): PDB ID code 1UZF [4], for the C domain (tACE) and PDB ID code 2C6N [6], for the N domain of sACE. All crystallographic water molecules, bound inhibitors and other heteroatoms with the exception of zinc and chloride ions were removed. Missing hydrogen atoms and heavy atoms were added using the XLEaP module of AMBER 9 [23]. The missing residues were added by manual placement of their  $\text{C}_\alpha$  atoms and subsequent automatic modelling of the remaining atoms using XLEaP. The protonation state of ionizable side chains was predicted by (i) the programme H++ using a continuum electrostatic model based on the Poisson–Boltzmann method [24] and (ii) visual inspection of all histidine residues to identify hydrogen-bonding networks with neighbouring residues. The system was initially relaxed with 500 steps of energy minimization using the steepest descent method and positional restraints with a harmonic force constant of 50 kcal/mol/Å<sup>2</sup> on all heavy atoms except those not determined in the X-ray structure. The generalized Born implicit solvation model GB<sup>HCT</sup> [25] was employed with a 16 Å cut-off for the non-bonded interactions. Ligands displayed in Scheme 2 were also treated with the united-atom approximation, and were prepared with the OpenEye suite of programmes using the AM1-BCC partial charge distribution [26].

#### Docking of the ligands

AutoDock 3.05 [27] was used for the docking calculations and AutoDockTools was used for visual inspection of the docking results. Protein and ligands were treated with the united-atom approximation by merging all non-polar hydrogens. Kollman

partial charges were assigned to all protein atoms, whereas for zinc and chloride ions formal charges and van der Waals parameters from the AMBER database were assigned. The sulfhydryl groups were set to be deprotonated, depending on their coordination to the catalytic zinc of ACE. The grid maps were centred on the ligand's binding site, with  $81 \times 81 \times 81$  grid points of 0.25 Å spacing. The Lamarckian genetic algorithm was employed with the following parameters: a population size of 250 individuals; a maximum number of  $5 \times 10^6$  energy evaluations and a maximum number of 27 000 generations; an elitism value of 1; a mutation rate of 0.02 and a crossover rate of 0.80 [27]. For all the calculations, 100 docking rounds were performed with step sizes of 0.2 Å for translations and  $5^\circ$  for orientations and torsions. Docked conformations were clustered with a 0.5 Å tolerance for the root mean square positional deviation. The protein–ligand complexes were visually inspected with AutoDockTools.

### Results and Discussion

Considering that the proline of the captopril fits into a hydrophobic binding pocket of the active site, it was supposed that increasing the hydrophobicity of this ligand moiety could improve its binding affinity. A few years ago, we designed a lipophilic analogue of proline, the silaproline [20], which exhibits an enhanced hydrophobicity and conserves structural feature [28–30]. We synthesized a silylated analogue of captopril **1**, the silacaptopril **2**, with a dimethylsilyl group replacing a methylene, which could improve hydrophobic interactions with ACE.

#### Synthesis

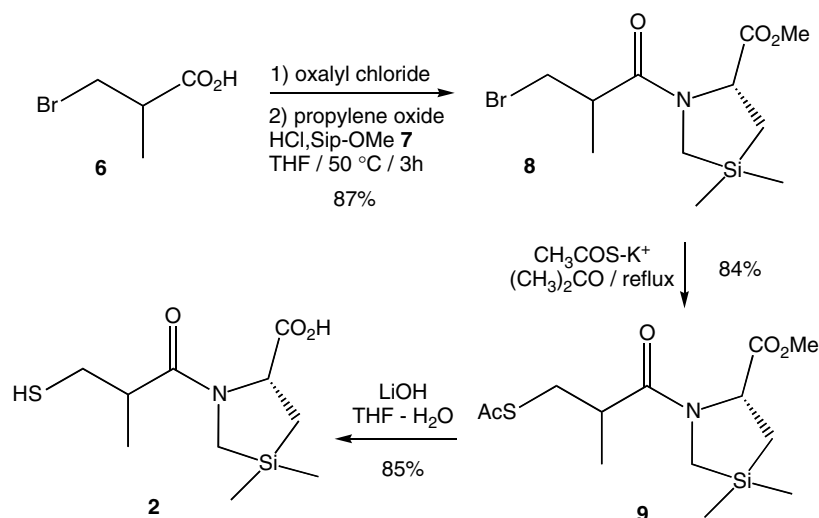
The 3-bromo-2-methylpropionic acid **6**, which is easily obtained by hydrobromination of methacrylic acid [31], was condensed with the methyl ester of silaproline **7**. Several coupling conditions have been tested, varying the reagents, the base and the solvent. Neither of coupling reagents classically employed in peptide synthesis (BOP, DCC/DMAP, DCC/HOBt, EDCl) gave satisfying results whatever bases and solvents were used. The intermediate **8** was finally obtained in 87% yield by activation of **6** with oxalyl chloride followed by coupling with the silaproline derivative **7** in the presence of propylene oxide. Subsequently, the bromide was substituted by potassium thioacetate in refluxing acetone to afford **9** in 84% yield. A final treatment with lithium hydroxide in a mixture of THF and water allowed the deprotection of both methyl ester and acetate to provide the silacaptopril **2** in 85% yield (Scheme 3).

#### Inhibitory Effect for ACE Activity

Inhibitory activities of captopril (0.1 nM–1  $\mu\text{M}$ ) and silacaptopril derivatives were determined at different concentrations (0.1 nM–0.1 mM) by using the optimized fluorimetric assay previously described (see Section Materials and Methods). ACE activity without addition of captopril or silacaptopril in the reaction mixture was set as 100%.

Captopril and silacaptopril (R/S,R) were both able to inhibit ACE activity completely (Figure 1). The evaluated IC<sub>50</sub> of captopril (6.3 nM) was highly coherent with data reported previously in the literature. Silacaptopril (R/S,R) with IC<sub>50</sub> value of 43 nM exhibited a lower inhibitory effect for ACE, compared to captopril.

The replacement of proline by silaproline did not affect the inhibition significantly, possibly indicating that hydrophobic



**Scheme 3.** Synthesis of silacaptopril.

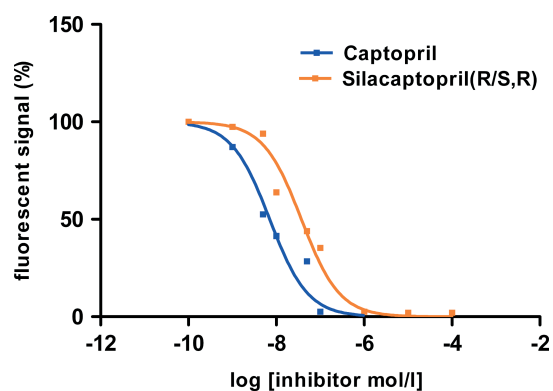


**Figure 1.** Inhibitory effect of captopril and silacaptopril on ACE activity.

interactions are not essential for the binding of silacaptopril to ACE. In addition, steric hindrance, which has increased significantly, might hamper binding site approach. Docking calculations can probe the binding properties of silacaptopril and its analogues.

### Active Site Nomenclature

In order to illustrate the enzyme active site and subsites of proteases that are susceptible to accommodating the peptide or substrate group, Schechter and Berger introduced in 1967 [32] a nomenclature using as an example the prototype of the papain family of cysteine peptidases. According to this nomenclature, the active site of the protease is divided into different subsites that may come into contact with the substrate. The protease subsites interacting with the *N*-terminus of the substrate are numbered  $S_1$ – $S_n$  (non-primed sites), whereas those that interact with the *C*-terminus are numbered as  $S'_1$ – $S'_n$  (primed sites). Accordingly, the position of the residues/groups of the substrate/inhibitor relative to the scissile bond is denoted as  $P_1$ – $P_n$ , and  $P'_1$ – $P'_n$ , respectively.

### ACE-captopril Simulated Docking Interactions

The recently reported crystal structures of human tACE [4] (C domain of sACE) and N domain of sACE [6] allowed the

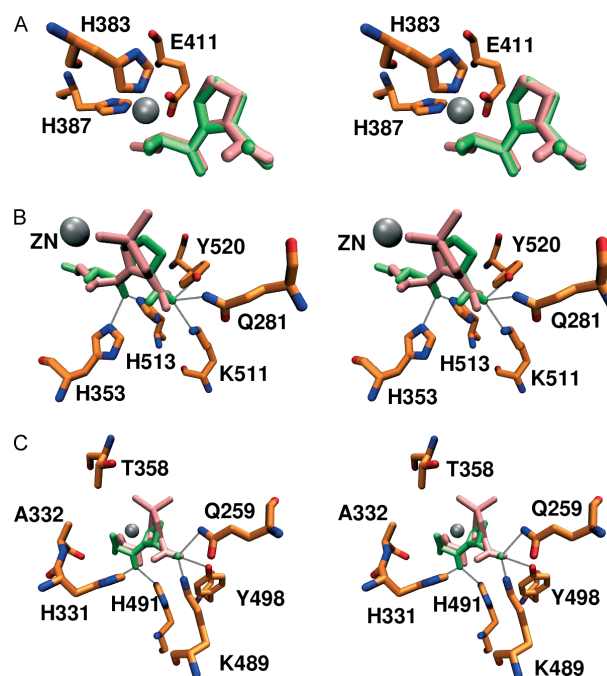


**Figure 2.** (A) Stereo representation of the cACE–captopril complex. The X-ray captopril (PDB ID 1UZF) and the simulated captopril are shown in pink and green, respectively. (B, C) Stereo representation of cACE and nACE in complex with captopril (green) and silacaptopril (pink). In A–C, the catalytic residues' carbon atoms are shown in orange and zinc as silver sphere.

prediction of small molecule or short peptide binding modes into the Zn-containing catalytic sites of the enzyme. The binding subsites  $S_1$ ,  $S'_1$  and  $S'_2$  are well characterized, and the differences at the active sites between the two domains of ACE are documented [6]. Based on the structure models of ACE, efforts were focused on the generation of the protein–ligand complexes through docking simulation approaches. The reference compound captopril, (2*R*)-1-[(2*S*)-2-methyl-3-sulfanyl-propanoyl]pyrrolidine-2-carboxylic acid, exhibits a remarkable preference for binding to the active site of both ACE domains. The compounds used

**Table 1.** Docking results for each ligand in complex with ACE

Ligand	cACE domain		nACE domain	
	Mean docked energy (kcal/mol)	Mean binding energy (kcal/mol)	Mean docked energy (kcal/mol)	Mean binding energy (kcal/mol)
Captopril	-10.47	-9.69	-9.11	-8.23
Silacaptopril	-10.50	-10.38	-12.02	-11.94
Analogue <b>3</b>	-9.24	-9.21	-10.54	-10.49
Analogue <b>4</b>	-9.66	-9.60	-11.00	-10.88
Analogue <b>5</b>	-10.22	-10.11	-11.10	-11.04

in this study are captopril **1** [15,18] and silacaptopril **2** (N-R-3-mercapto-2-methylpropanoyl-L-silaproline), which are derived from the replacement of the proline of captopril with 4'-dimethylsilaproline [20] (Scheme 2). Variation on silicon atom substitution has been introduced to evaluate the importance of steric hindrance at these positions (analogues **3**, **4** and **5**, Scheme 2). AutoDock was able to predict the conformation of captopril bound to cACE within 1.22 Å root mean square deviation (Figure 2A) as the top ranked solution with the lowest binding free energy, indicating the ability of the method to predict a proper conformation. All analogues exhibited binding energies ranging from -8.0 to -11.0 kcal/mol, with silacaptopril exhibiting the lowest docking energy in both ACE domains (Table 1). In addition, docking results reveal that all the compounds adopted similar orientations into the ACE ligand binding site.

#### ACE C Domain (cACE) Contacts with Captopril and Silacaptopril

Structural analysis of the cACE–captopril X-ray complex reveals the important ACE residues for interaction with captopril and for accommodation of the ligand into the binding site [16]. The major interactions between cACE residues and captopril are summarized in Table 2. Captopril's deprotonated sulfhydryl group interacts directly with the catalytic Zn<sup>2+</sup> ion (2.32 Å), the carbonyl group between the sulfhydryl group, and the terminal proline is positioned by two strong hydrogen bonds from the two histidines (His 513 and His 353) and one oxygen of the proline moiety carboxylate group is held by interactions with Tyr 520, Gln 281 and Lys 511.

We have carried out docking simulation approaches in order to examine the interactions of cACE residues with silacaptopril. Analysis of the docking simulations data reveals that the orientation of the most favoured docking conformation of silacaptopril in the binding site of cACE is rather similar to that of captopril (Figure 2B), with a similar strong interaction between the catalytic Zn<sup>2+</sup> ion and the sulfhydryl group of silacaptopril (2.25 Å). In addition, similar to captopril, electrostatic interactions are formed between the central carbonyl group of silacaptopril and the histidines His353 and His513. Similarly, an oxygen atom of the proline moiety carboxylate group exhibits electrostatic interactions with Gln281, Lys511 and Tyr520.

Furthermore, S<sub>1</sub>' and S<sub>2</sub>' subsites of cACE domain accommodate the proline analogue moiety of silacaptopril into a hydrophobic cage comprising residues Val380, Phe457, Phe527, Tyr523 and Ala354 (Table 2). The hydrophobic and van der Waals interactions between cACE–captopril and cACE–silacaptopril are similar, with one exception. It is interesting to note that, in contrast to

captopril, Val380 displays favourable hydrophobic interactions with the proline moiety of silacaptopril, probably due to the two coordinating methyl groups of Si. These additional interactions of Val380 might contribute to the better binding energies of cACE with silacaptopril (Table 1). This is probably due to the limited accuracy of the AutoDock scoring function, which has a residual error of 2.18 kcal/mol [27]. The predicted binding affinities of the lowest energy docked conformations, using the LGA method and the new empirical free energy function, were within the standard residual error of the force field for captopril and silacaptopril. Therefore, a straightforward comparison of the two ligands based exclusively on their predicted binding energy could not explain which one is a more potent inhibitor of ACE, and thus more experimental data are needed.

#### ACE N Domain (nACE) Contacts with Captopril and Silacaptopril

Similarly, docking simulation approaches were performed in order to examine the interactions of nACE residues with both captopril and silacaptopril. Several key interactions indicative of positioning and binding of the ligands into the binding site of nACE domain are summarized in Table 2. The zinc ion is coordinated by the sulfhydryl group (2.31 and 2.44 Å for captopril and silacaptopril, respectively), as in the case of cACE with captopril. It is noteworthy that captopril and silacaptopril orient one oxygen of the proline moiety carboxylate group in a way that favours interactions with Gln259, Lys489 and Tyr498, similarly to the cACE domain and residues Gln281, Lys511 and Tyr520 (Figure 2C). Furthermore, the central carbonyl group of both captopril and silacaptopril forms two hydrogen bonds with histidines His331 and His491.

Several C domain active site residues differ in the corresponding N domain sequence. An important difference is the alteration of Val380 to Thr358. The central methyl group of captopril displays van der Waals contacts with Thr358 (nACE), in contrast with Val380 of cACE, which does not exhibit strong interactions with captopril. This could be attributed to the fact that the side-chain of Val380 is distant from the central methyl group.

On the other hand, the methyl groups of 4'-dimethylsilaproline exhibit favourable hydrophobic contacts with Val380 (cACE) and Thr358 (nACE). One of the methyl groups of 4'-dimethylsilaproline displays additional favourable hydrophobic interactions with Phe505, a contact that is not observed in the nACE–captopril complex. These contacts in the simulated complex of cACE–silacaptopril might be crucial for the lowest binding/docking energy. In addition, several hydrophobic and van der Waals contacts are present in the S<sub>1</sub>' and S<sub>2</sub>' subsites of nACE, comprising residues Thr358, Phe435, Phe505, Tyr501, His331, His361 and Ala332 (Table 2).

#### cACE and nACE Catalytic Site Interactions with the Silacaptopril Analogues

As far as the contacts of silacaptopril analogues (Scheme 2) with cACE and nACE are concerned, the docking simulations display some minor contact differences with the interactions that are observed between cACE/nACE and silacaptopril. Specifically, the central carbonyl group of analogue **3** is being oriented to an opposite way regarding the orientation of silacaptopril in the binding site of cACE. Furthermore, the ethyl groups of silicon exhibit favourable hydrophobic contacts with residues Phe457 and Phe527 but, opposed to silacaptopril, the ethyl group does

**Table 2.** cACE and nACE residues that exhibit major electrostatic and hydrophobic interactions with captopril and silacaptopril

	cACE domain		nACE domain	
	Electrostatic interactions	Hydrophobic interactions	Electrostatic interactions	Hydrophobic interactions
Captopril	Gln281, Lys511, Tyr520, His513, His353	Tyr523, Phe457, Tyr523	Gln259, Lys489, Tyr498, His331, His491	Thr358, Tyr501, Ala332, His331, His361
Silacaptopril	Gln281, Lys511, Tyr520, His513, His353	Tyr523, Val380, Phe527, Tyr523	Gln259, Lys489, Tyr498, His331, His491	Thr358, Tyr501, Phe505, Ala332, His331, His361

not exhibit hydrophobic interactions with Val380 due to the different orientation.

Concerning analogue **4**, the only observed differences are the stronger hydrophobic interactions of the methyl/ethyl groups of silicon displayed with Tyr523 and Phe527 respectively, and the proline moiety van der Waals interactions with Phe457. As far as the analogue **5** is concerned, the differences of the most energetically favourable conformation with regard to the silacaptopril are the hydrophobic interactions of the silicon ethyl group with Ala354 and Val380, the proline van der Waals interactions with His353 and the central methyl group hydrophobic interactions with Phe527.

## Conclusions

In the present study, docking simulations were used to analyze interactions between the ACE active site and silacaptopril as well as interactions between ACE and silacaptopril analogues, in order to predict the structural factors that might contribute significantly to their binding. It should be noted that the choice of the most favoured docking conformations of captopril and silacaptopril for binding in the catalytic site of ACE was ultimately dictated by its final binding energy and the orientation of the ligand. Data analysis reveals that silacaptopril/analogues exhibited affinity in the same range as captopril and displayed great similarity regarding the orientation of captopril in complex with ACE. Thus the substitution of the proline moiety with silaproline did not affect considerably the inhibition properties of the parent molecule, although the silacaptopril exhibits slightly higher IC<sub>50</sub> than captopril. Nevertheless, the silacaptopril analogue may benefit from the presence of silaproline by exhibiting increased biodisponibility and resistance towards enzyme degradation.

## References

- Hubert C, Houot AM, Corvol P, Soubrier F. Structure of the angiotensin I-converting enzyme gene. Two alternate promoters correspond to evolutionary steps of a duplicated gene. *J. Biol. Chem.* 1991; **266**: 15377–15383.
- Ehlers MR, Fox EA, Strydom DJ, Riordan JF. Molecular cloning of human testicular angiotensin-converting enzyme: the testis isozyme is identical to the C-terminal half of endothelial angiotensin-converting enzyme. *Proc. Natl Acad. Sci. USA* 1989; **86**: 7741–7745.
- Soubrier F, Alhenc-Gelas F, Hubert C, Allegrini J, John M, Tregear G, Corvol P. Two putative active centers in human angiotensin I-converting enzyme revealed by molecular cloning. *Proc. Natl Acad. Sci. USA* 1988; **85**: 9386–9390.
- Natesh R, Schwager SL, Sturrock ED, Acharya KR. Crystal structure of the human angiotensin-converting enzyme-lisinopril complex. *Nature* 2003; **421**: 551–554.
- Watermeyer JM, Sewell BT, Schwager SL, Natesh R, Corradi HR, Acharya KR, Sturrock ED. Structure of testis ACE glycosylation mutants and evidence for conserved domain movement. *Biochemistry* 2006; **45**: 12654–12663.
- Corradi HR, Schwager SL, Nchinda AT, Sturrock ED, Acharya KR. Crystal structure of the N domain of human somatic angiotensin I-converting enzyme provides a structural basis for domain-specific inhibitor design. *J. Mol. Biol.* 2006; **357**: 964–974.
- Redelinghuys P, Nchinda AT, Sturrock ED. Development of domain-selective angiotensin I-converting enzyme inhibitors. *Ann. N Y Acad. Sci.* 2005; **1056**: 160–175.
- Spyroulias GA, Cordopatis P. Current inhibition concepts of zinc metalloproteinases involved in blood pressure regulation. *Curr. Enzyme Inhibit.* 2005; **1**: 29–42.
- Shapiro R, Holmquist B, Riordan JF. Anion activation of angiotensin converting enzyme: dependence on nature of substrate. *Biochemistry* 1983; **22**: 3850–3857.
- Papakyriakou A, Spyroulias GA, Sturrock ED, Manessi-Zoupa E, Cordopatis P. Simulated interactions between angiotensin-converting enzyme and substrate gonadotropin-releasing hormone: novel insights into domain selectivity. *Biochemistry* 2007; **46**: 8753–8765.
- Thorsett ED, Harris EE, Aster SD, Peterson ER, Snyder JP, Springer JP, Hirshfield J, Tristram EW, Patchett AA, Ulm EH, Vassil TC. Conformationally restricted inhibitors of angiotensin converting enzyme: synthesis and computations. *J. Med. Chem.* 1986; **29**: 251–260.
- Fournie-Zaluski MC, Coric P, Turcaud S, Lucas E, Noble F, Maldonado R, Roques BP. "Mixed inhibitor-prodrug" as a new approach toward systemically active inhibitors of enkephalin-degrading enzymes. *J. Med. Chem.* 1992; **35**: 2473–2481.
- Roques BP, Noble F, Crine P, Fournie-Zaluski MC. Inhibitors of neprilysin: design, pharmacological and clinical applications. *Meth. Enzymol.* 1995; **248**: 263–283.
- Wyvrat MJ, Patchett AA. Recent developments in the design of angiotensin-converting enzyme inhibitors. *Med. Res. Rev.* 1985; **5**: 483–531.
- Ondetti MA, Rubin B, Cushman DW. Design of specific inhibitors of angiotensin-converting enzyme: new class of orally active antihypertensive agents. *Science* 1977; **196**: 441–444.
- Natesh R, Schwager SL, Evans HR, Sturrock ED, Acharya KR. Structural details on the binding of antihypertensive drugs captopril and enalaprilat to human testicular angiotensin I-converting enzyme. *Biochemistry* 2004; **43**: 8718–8724.
- Mutahi M, Nittoli T, Guo L, Sieburth SM. Silicon-based metalloprotease inhibitors: synthesis and evaluation of silanol and silanediol peptide analogues as inhibitors of angiotensin-converting enzyme. *J. Am. Chem. Soc.* 2002; **124**: 7363–7375.
- Cushman DW, Cheung HS, Sabo EF, Ondetti MA. Design of potent competitive inhibitors of angiotensin-converting enzyme. Carboxyalkanoyl and mercaptoalkanoyl amino acids. *Biochemistry* 1977; **16**: 5484–5491.
- Hanessian S, Reinhold U, Saulnier M, Claridge S. Probing the importance of spacial and conformational domains in captopril analogs for angiotensin converting enzyme activity. *Bioorg. Med. Chem. Lett.* 1998; **8**: 2123–2128.
- Vivet BCF, Martinez J. Synthesis of silaproline, a new proline surrogate. *Eur. J. Org. Chem.* 2000; **5**: 807–811.
- Santos RA, Krieger EM, Greene LJ. An improved fluorometric assay of rat serum and plasma converting enzyme. *Hypertension* 1985; **7**: 244–252.

- 22 Mehanna AS, Dowling M. Liquid chromatographic determination of hippuric acid for the evaluation of ethacrynic acid as angiotensin converting enzyme inhibitor. *J. Pharm. Biomed. Anal.* 1999; **19**: 967–973.
- 23 Case DADT, Cheatham TE III, Simmerling CL, Wang J, Duke RE, Luo R, Merz KM Jr, Pearlman DA, Crowley M, Walker RC, Zhang W, Wang B, Hayik S, Roitberg A, Seabra G, Wong KF, Paesani F, Wu X, Brozell S, Tsui V, Gohlke YL, Tan CH, Mongan J, Hornak V, Cui G, Beroza P, Mathews DH, Schafmeister C, Ross WS, Kollman PA. *AMBER 9*. University of California: San Francisco, 2006.
- 24 Bashford D, Karplus M. pKa's of ionizable groups in proteins: atomic detail from a continuum electrostatic model. *Biochemistry* 1990; **29**: 10219–10225.
- 25 Tsui VCD. Theory and applications of the generalized Born solvation model in macromolecular simulations. *Biopolymers* 2001; **56**: 275–291.
- 26 Jakalian A, Jack DB, Bayly CI. Fast, efficient generation of high-quality atomic charges. AM1-BCC model: II. Parameterization and validation. *J. Comput. Chem.* 2002; **23**: 1623–1641.
- 27 Morris GM, Goodsell DS, Halliday RS, Huey R, Hart WE, Belew RK, Olson AJ. Automated docking using a Lamarckian genetic algorithm and an empirical binding free energy function. *J. Comput. Chem.* 1998; **19**: 1639–1662.
- 28 Vivet B, Cavelier F, Martinez J, Didierjean C, Marraud M, Aubry A. A silaprolin-containing dipeptide. *Acta Crystallogr. C* 2000; **56**: 1452–1454.
- 29 Cavelier F, Vivet B, Martinez J, Aubry A, Didierjean C, Vicherat A, Marraud M. Influence of silaprolin on peptide conformation and bioactivity. *J. Am. Chem. Soc.* 2002; **124**: 2917–2923.
- 30 Cavelier F, Marchand D, Martinez J, Sagan S. Biological activity of silylated amino acid containing substance P analogues. *J. Pept. Res.* 2004; **63**: 290–296.
- 31 Nam DH, Lee CS, Ryu DD. An improved synthesis of captopril. *J. Pharm. Sci.* 1984; **73**: 1843–1844.
- 32 Schechter I, Berger A. On the size of the active site in proteases. I. Papain. *Biochem. Biophys. Res. Commun.* 1967; **27**: 157–162.